Journal of Structural Geology, Vol. 15, Nos 3–5, pp. 465 to 475, 1993
Printed in Great Britain

0191–8141/93 $06.00+0.00

Variation in quartz arenite deformation mechanisms between a roof sequence and duplexes

CHARLES M. ONASCH

Department of Geology, Bowling Green State University, Bowling Green, OH 43403, U.S.A.

and

WILLIAM M. DUNNE

Department of Geological Sciences, University of Tennessee, Knoxville, TN 37996, U.S.A.

(*Received* 27 *December* 1991; *accepted in revised form* 3 *September* 1992)

Abstract—Microstructural abundances and histories in quartz arenite of the Lower Silurian Tuscarora Sandstone were used to determine the nature and role of microscale deformation in a cover sequence and underlying thrust system, and to assess the degree to which the cover sequence accommodated emplacement of the thrust system. Sandstone samples are located across the transition from the central to southern Appalachian foreland thrust system where the thrusts change from blind to emergent southwards and where southern deformation of early Alleghanian age has been previously shown to be overprinted by central deformation of Alleghanian age. Microstructures observed with transmitted light and cathodoluminescence microscopy indicate that grain-scale deformation occurred by dislocation flow, pressure solution, and microfracturing, with the last being generally the most important. The sequence of deformation mechanisms is the same for the cover sequence and the thrust system: pressure solution during sedimentary compaction; dislocation flow during layer-parallel shortening; and localized microfracturing with limited pressure solution near major thrust ramps and in steep fold limbs. A greater abundance of dislocation flow microstructures in the cover sequence from layer-parallel shortening indicates grain-scale accommodation in the Tuscarora Sandstone of some shortening associated with emplacement of the thrust system. The transition zone between the central and southern Appalachians contains the greatest occurrence of every microstructure which is consistent with the area having been affected by diachronous central and southern Alleghanian deformations.

INTRODUCTION

BLIND thrust systems are a major component of foreland-style deformation in many orogenic belts of the world (Dunne & Ferrill 1988). Although geometrically similar to emergent systems with imbricate fans and duplexes, blind systems differ in that the active faults remain in the subsurface beneath a pretectonic cover, or roof sequence, of sedimentary rocks (Thompson 1979, Boyer & Elliott 1982). A major problem in understanding the evolution of blind foreland thrust systems is determining the means by which the roof sequence accommodates emplacement of the underlying thrust system. The roof sequence must accommodate the shortening in the thrust system without becoming incorporated into the macroscale fault network.

Previous investigations (Mitra 1987, Geiser 1988a, Ferrill & Dunne 1989, Meyer & Dunne 1990) have shown that roof sequences accommodate at least some of the shortening by deformation at the microscale. Layer-parallel shortening in advance of blind thrusting, passive macrofolding above growing thrust-related folds and active parasitic buckling, and locally intense deformation where fold limbs overturn or thrust faults develop all can result in significant internal strains. Although the thrust system can be thought of as a series of rigid blocks, other studies (Elliott 1976, Sanderson 1982, Marshak & Engelder 1985, Woodward *et al.* 1986, Evans & Dunne 1991, Wu & Groshong 1991) have shown that foreland thrust sheets deform at the microscale as well, accommodating layer-parallel shortening in advance of and during sheet formation, ramp formation possibly with fault-propagation folding, distributed shear during displacement, and horizontal flattening during the formation of younger sheets.

Microstructures are a primary means for identifying the operative mechanisms, rock rheology, kinematics and dynamics during deformation (Knipe 1989). Although the use of microstructures has become commonplace in structural analysis, there still is a lack of quantitative data on the occurrence of microstructures and their variation in different structural settings. In the absence of recrystallization, the relative abundance of different microstructures at a single location is a measure of the relative importance of competing deformation mechanisms at that location, whereas the variation in abundance between locations is an indication of how the importance of the mechanisms varies spatially. The different strain histories of the roof sequence and thrust system and the degree to which these strains occur by microscale deformation may be reflected as differences in the microstructural histories and abundances.

Furthermore, any microscale accommodation in the roof sequence of faulting in the blind thrust system should also be evident in microstructural abundances.

The purpose of this paper is to determine the nature and role of microscale deformation in both the cover and underlying thrust system and to assess the degree to which the roof sequence accommodates emplacement of the thrust system. The approach in this study is to examine a single lithology in a single stratigraphic unit that passes laterally from thrust system to roof sequence. This approach minimizes lithologic effects and isolates the structural effects related to differing deformational conditions (P, T, $\dot{e}$, etc.) and histories associated with different locations in the roof sequence or thrust system.

Geologic setting

The Appalachian foreland fold and thrust belt, which extends some 1400 km along strike from New York to Alabama, is divided into central and southern segments by a major reentrant located in Virginia. This tectonic juncture is marked by a change from macrofolds trending about 030° in the central Appalachians to major thrust faults trending about 060° in the southern Appalachians (Rodgers 1970, Dean *et al.* 1988) (Fig. 1). The juncture is a transition zone (between bold dotted lines, Fig. 1a) where macrofolds and thrusts have an intermediate trend of 045–050°. The presence of a roof sequence (Fig. 1) is a function of the existence of a roof thrust above the thrust sheets, which are composed of Cambro-Ordovician carbonates (Perry 1978, Woodward 1985, Kulander & Dean 1986, 1988). The roof thrust is located in the shale-dominated Middle Ordovician Martinsburg Formation, but disappears southward (Fig. 1) as this or equivalent units thin laterally into a more competent, limestone and sandstone-dominated sequence (Colton 1970, Diecchio 1985, Kreisa & Springer 1987).

The Lower Silurian Tuscarora Sandstone occurs in the roof sequence of the central Appalachians (Section A, Fig. 1b) and in the thrust system in the southern Appalachians (Section H, Fig. 1b). In the transition zone, it is in both the roof and the thrust system (Section C, Fig. 1b). The lithotectonic transition of the Tuscarora Sandstone from roof to duplex does not exactly correspond with the tectonic juncture between the central and southern Appalachians (Fig. 1a).

The tectonic juncture also represents a difference in deformation age between the southern and central Appalachians. Both areas were deformed during the Alleghanian orogeny, but deformation in the southern Appalachians is older (Geiser & Engelder 1983, Dean *et al.* 1988). Overprinting relationships between stylolites, cleavage and fault slickenlines in the Appalachian Plateau adjacent to the transition zone show this sequence of deformation (Dean *et al.* 1988).

The Tuscarora Sandstone is a medium-grained, framework-supported quartz arenite with beds 30–200 cm thick and a total thickness of 30–100 m. In the central Appalachians, the sandstone was buried to 6 km by Pennsylvanian times, whereas in the southern Appalachians, burial was to only 4 km (Reger & Price 1926, Tilton *et al.* 1927, Colton 1970, Bartholomew 1987). Burial depth and conodont color-alteration indices (Epstein *et al.* 1977, Harris 1979) in adjacent limestones indicate that the Tuscarora Sandstone was deformed during the Alleghanian orogeny at about 150–250°C. In the southern Appalachian foreland, burial depth, conodont color-alteration indices, and vitrinite reflectance in Mississippian coals (Lewis & Hower 1990) indicate that the temperature during deformation for the Tuscarora Sandstone was somewhat lower, and increased towards the hinterland from 120 to 200°C.

Methods

Seventy-five samples were collected along seven strike-normal traverses (Fig. 1). Care was taken to avoid effects of local deformation by sampling only outcrops lacking minor folds or faults. Thin sections from the samples, cut normal to bedding and parallel to dip, were examined in both transmitted light and cathodoluminescence. The latter has proven useful in identifying certain microfractures and pressure solution features, relative age relations between microstructures and diagenetic cements, and the origin of certain microfabrics (Sprunt & Nur 1979, Blenkinsop & Rutter 1986, Narahara & Wiltschko 1986, Onasch 1990).

Microstructural abundances, % matrix (clay), % cement and grain size were determined by point-counting 250 grains per section. Assuming random occurrence of the features being counted, the errors at a 95% confidence level associated with 10, 20 and 50 volume % are 4, 5 and 6%, respectively (Van Der Plas & Tobi 1965). If a binomial distribution of features is assumed, the errors are 2.5, 3 and 3.7%, respectively (Koch & Link 1970). Microstructural histories were integrated from the relative age relationships between microstructures in a number of thin sections.

MICROSTRUCTURES

Grain-scale deformation in the Tuscarora was accommodated by three mechanisms: (1) dislocation flow; (2) pressure solution; and (3) microfracturing. Microstructures related to dislocation flow include undulatory and patchy extinction (Fig. 2a), deformation lamellae and deformation bands (Fig. 2b). Undulatory extinction was differentiated from patchy extinction on the basis of the sweeping extinction in the former and sharply domainal extinction in the latter. Patchy extinction can be a manifestation of polygonization and subgrain formation (Nicolas & Poirier 1976), but can also result from microfracturing (Tullis & Yund 1987). Deformation lamellae, also known as Fairbairn lamellae (Groshong 1988, after Fairbairn 1941), are defined by parallel zones of differing birefringence which are sometimes decorated with minute brownish inclusions. Lamellae orientations were not measured in this study, but in the same

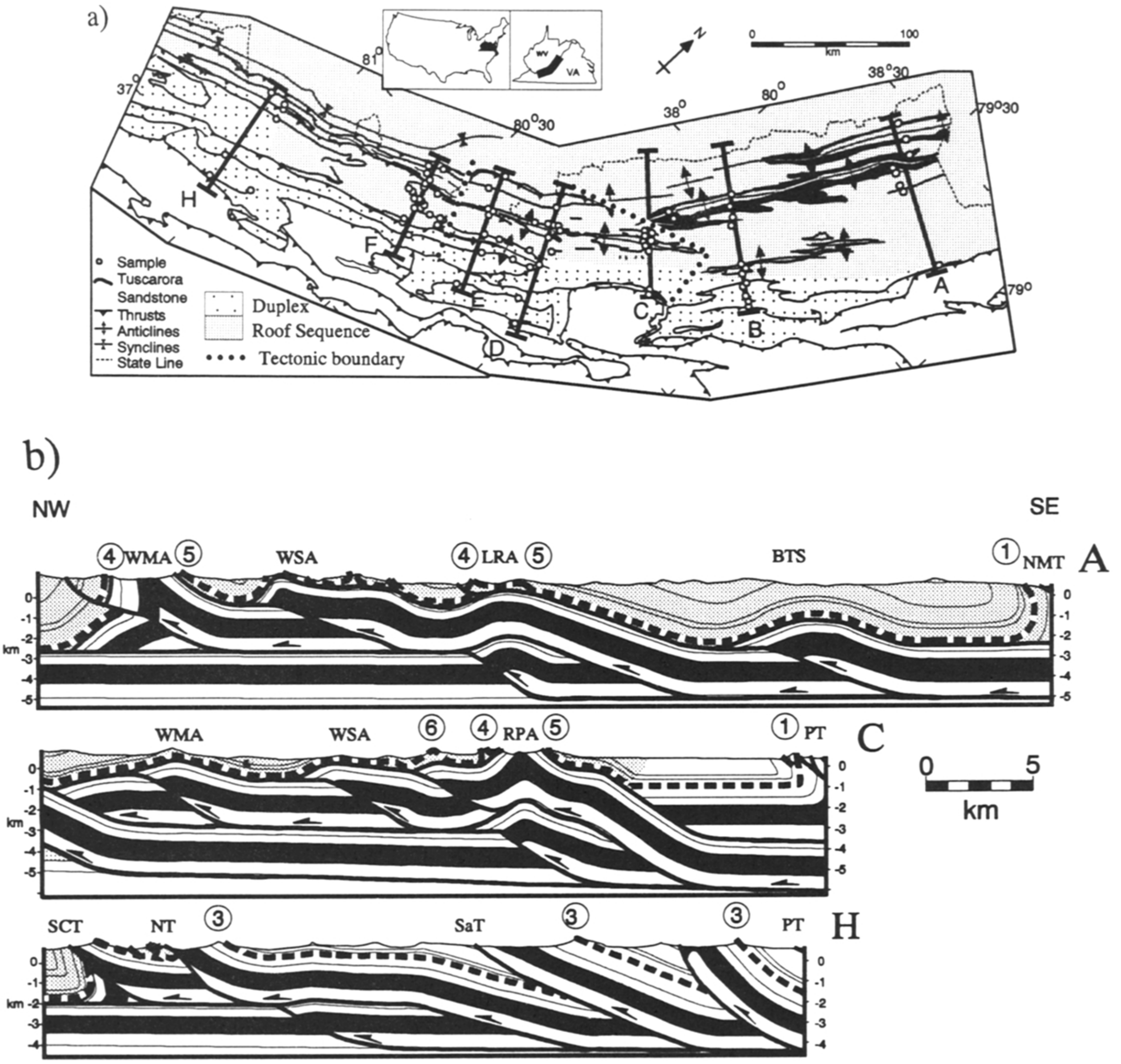

Fig. 1. (a) Map of distribution of major faults, major folds, and the Tuscarora Sandstone at the juncture of the southern and central Appalachian foreland, showing where sandstone is in the roof sequence above the blind duplex and where it is in the duplex. Single capital letters designate sample lines (bold straight lines with nearby sample dots). (b) Cross-sections along sections A, C and H illustrate change of lithotectonic position for the Tuscarora Sandstone (bold dashed line) from roof sequence (light stipple) to incorporation into thrust sheets containing the Cambro-Ordovician carbonates (black and adjacent units). LRA—Long Ridge anticline; NMT—North Mountain thrust; NT—Narrows thrust; PT—Pulaski thrust; RPA—Ridge Patch anticline; SaT—Saltville thrust; SCT—St Clairs thrust; WMA—Wills Mountain anticline; and WSA—Warm Spring anticline. Numbers refer to structural locations described in text. Modified from Reger & Price (1926), Tilton *et al.* (1927), Reger (1931), Butts (1940), Cooper (1944), Bick (1960, 1962), Calver (1960), Spencer (1964), Kozak (1965, 1970), Rader (1967, 1969), McGuire (1970, 1976), Amato (1974), Bartholomew & Lowery (1979), Bartholomew (1981, 1987) and Schultz *et al.* (1986).

unit 100 km to the north lamellae have a sub-basal orientation (Onasch 1984). Deformation bands are 10–100 mm wide tabular, high strain zones where the crystal lattice has been rotated up to 30°. The bands commonly are subnormal to deformation lamellae where they occur in the same grain (Fig. 2b).

Pressure solution microstructures include sutured and interpenetrated grain boundaries (Fig. 2c) and, less commonly, transgranular solution surfaces or stylolites (Fig. 2d). All were counted as a single microstructure. Transgranular solution surfaces are evident only where the clay matrix exceeds 10%.

Textures diagnostic of microfracturing include fluid inclusion planes (FIPs) (Fig. 2e), microveins (Figs. 2f & g) and cataclastic bands (Fig. 3a). FIPs are healed microfractures decorated by fluid inclusions 0.5–4 mm in diameter. They are most commonly transgranular and occur in single or multiple orthogonal sets. Microveins are transgranular microfractures up to 200 mm in width filled with quartz in optical continuity with wall rock grains. They are difficult or impossible to detect with transmitted light microscopy, but are clearly visible in cathodoluminescence (compare Figs. 2f & g). No evidence for shear displacement was observed parallel to either FIPs or microveins; therefore, both are Mode I cracks. Cataclastic bands are discordant, tabular, subplanar zones of fine-grained quartz. They are also known as microfaults (Jamison & Stearns 1982), microbreccia-cataclastic zones (Lloyd & Knipe 1992) and deformation bands (Aydin & Johnson 1978), in all cases interpreted to be shear zones variably filled with cataclasite. In some Tuscarora samples, displacement parallel to the band could be proven. In others, offset of pre-existing features showed only extension with no shear, demonstrating that some apparent cataclastic bands are actually dilational microveins with a fine-grained fill.

Several samples, when viewed in transmitted light, contained linear bands in which the grains had textures ranging from serrated boundaries to a mortar texture (Fig. 3b). Based on grain morphology, these textures are similar to those commonly ascribed to recrystallization by grain boundary migration or subgrain rotation (Tullis & Yund 1985, Hirth & Tullis 1992). However, when the Tuscarora samples are examined in cathodoluminescence, the linear bands are dully luminescent microveins (Fig. 3c) in which the grains defining the texture were precipitated. Therefore, the textures formed by brittle failure and not dynamic rotational or migrational recrystallization. Sandstones or meta-sandstones containing serrated or mortar textures, especially where confined to linear bands, should be examined in cathodoluminescence before ascribing the textures to recrystallization.

Microstructures were assumed to have formed *in situ*, not inherited from source rocks. This assumption is valid for transgranuanular features such as FIPs, microveins, cataclastic bands, transgranular solution surfaces; and for features that were found to transect detrital grain-overgrowth cement contacts such as deformation lamellae, deformation bands and sutured grain boundaries. In addition, consistent orientations of shortening directions from deformation lamellae and bands in equivalent units elsewhere in the central Appalachian foreland (Perry 1968, Onasch & Canich 1976, Onasch 1984) argue that these microstructures are not inherited. Only undulatory and patchy extinction could not be shown unequivocally to have developed *in situ*. Neither of these, however, was used in assessing the amount of dislocation flow.

Relative ages of microstructures

The progression of microstructures, as determined by relative age relations, reflects the changes in rock rheology caused by changing deformational conditions (*P*, *T*, $\dot{e}$, etc.) (Knipe 1989, 1990). In the Tuscarora Sandstone, relative age relationships between microstructures indicate that these changes were similar for all samples, regardless of their structural location. Samples showing the complete microstructural history are rare; more commonly, the history was determined by integrating relations seen in a number of samples. Although most samples contained only fragments of the complete history, they formed an excellent consensus.

The oldest microstructures in all sandstone samples (Table 1) are sutured grain contacts and bedding-parallel, transgranular stylolites. These are followed by deformation lamellae and bands, and undulatory and patchy extinction. Deformation lamellae and bands often occur together, but the lamellae must be slightly older because they are rotated within bands (Fig. 2b). Next youngest structures are microfractures which cut deformation lamellae (Fig. 3d), cross deformation bands without deflection (Fig. 3e), truncate compaction-related transgranular solution surfaces, and offset grains containing deformation lamellae and bands (Fig. 3a). The parallelism between FIPs and microveins indicates that they are coeval, but some microveins are a little younger because they lack the inclusions that decorate FIPs (Fig. 3f). Cataclastic bands span the formation of FIPs and microveins. The youngest microstructures are transgranular, bedding-parallel solution surfaces which were found only in steeply-dipping limbs of macro-anticlines. Although these surfaces are parallel to the compaction-related solution surfaces, they are younger because they cut microfractures and locally cause rotation of microfractured rock (Fig. 3g). Previous studies (Sibley & Blatt 1976, Houseknecht 1988) of the diagenetic evolution of the Tuscarora Sandstone argued that the pressure solution fabric records only lithification and not tectonism. The clear age relations described above demonstrate that some solution in the Tuscarora Sandstone is of tectonic origin and not entirely diagenetic.

The microstructural history just described can be correlated to regional structural events using the orientation of microstructures and their preferential development in different structural settings. The first generation of solution surfaces formed by pressure solution during diagenetic compaction of the Tuscarora Sandstone (Table 1) (Sibley & Blatt 1976, Houseknecht 1988). These structures are subparallel to bedding, reflecting the vertically-dominated load during compaction. Deformation lamellae and bands formed during layer-parallel shortening, based on their correlation with similar features analyzed elsewhere in the central Appalachians which record layer-parallel shortening (Perry 1968, Onasch & Canich 1976, Onasch 1984). Such an interpretation here is consistent with layer-parallel shortening being the oldest penetrative tectonic deformation in both roof sequences and blind thrust systems throughout the Appalachian foreland (Table 1) (Geiser 1988a,b, Ferrill & Dunne 1989, Evans & Dunne 1991, Gray & Mitra 1991, Stamatakos & Kodama 1991). Unlike the compaction-related solution structures and dislocation flow structures, which served similar purposes in all structural settings, microfractures locally accommodated different structural events in the roof sequence and duplex (Table 1). In the duplex, microfractures in samples from within 200 m of hanging wall and footwall ramps (1 in Fig. 1b) have a variety of geometries, indicating that locally multiple failure modes were used to accommodate ramp formation. In the roof sequence, microfractures are well developed in

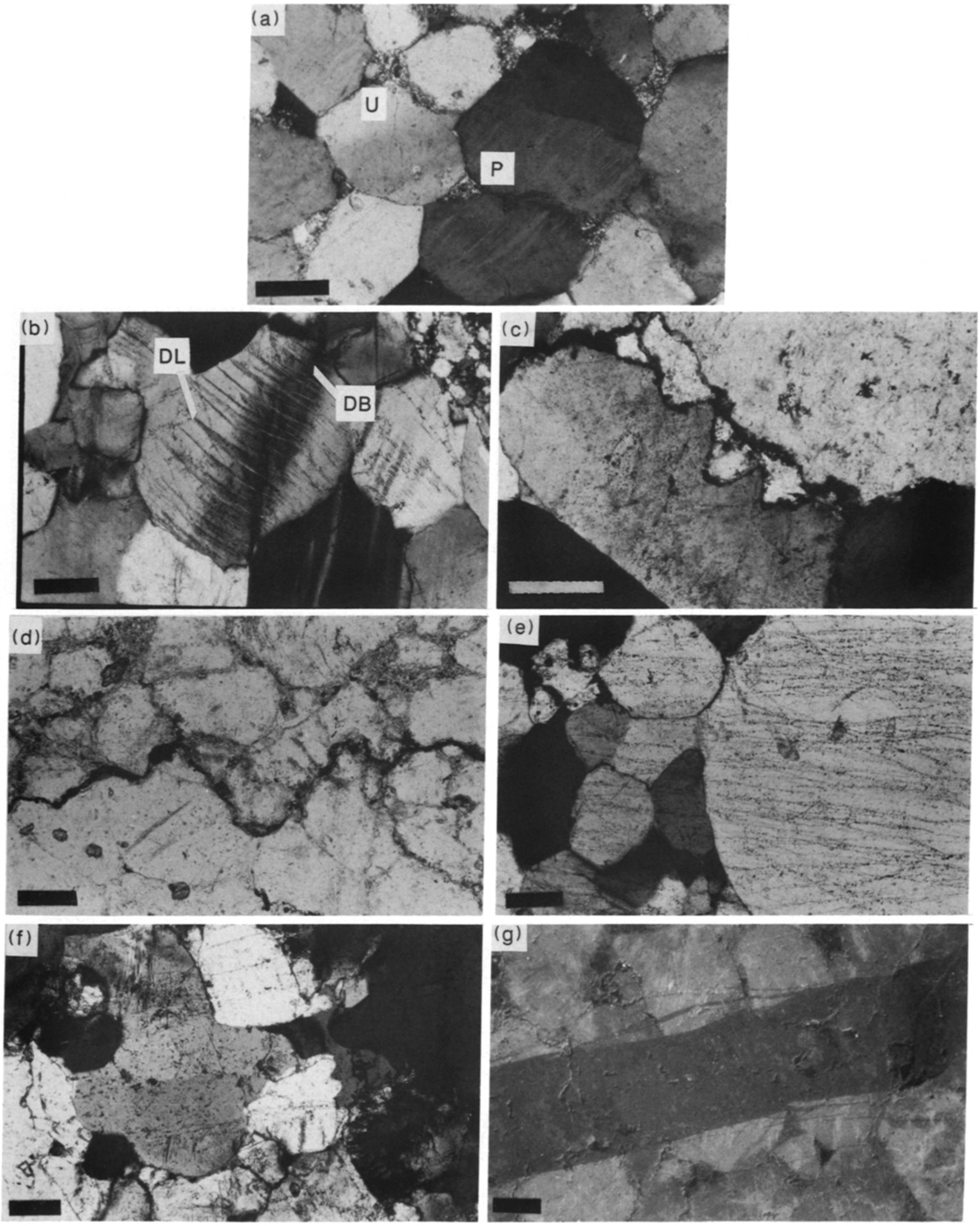

Fig. 2. Microstructures and microstructural relations in the Tuscarora Sandstone. (a) Undulatory (U) and patchy (P) extinction; (b) deformation lamellae (DL) that are rotated in a deformation band (DB); (c) sutured grain contact; (d) transgranular stylolite; (e) fluid inclusion planes (FIPs); (f) microvein in polarized light; and (g) the same microvein in cathodoluminescence. Scale bar in each photomicrograph is 0.1 mm.

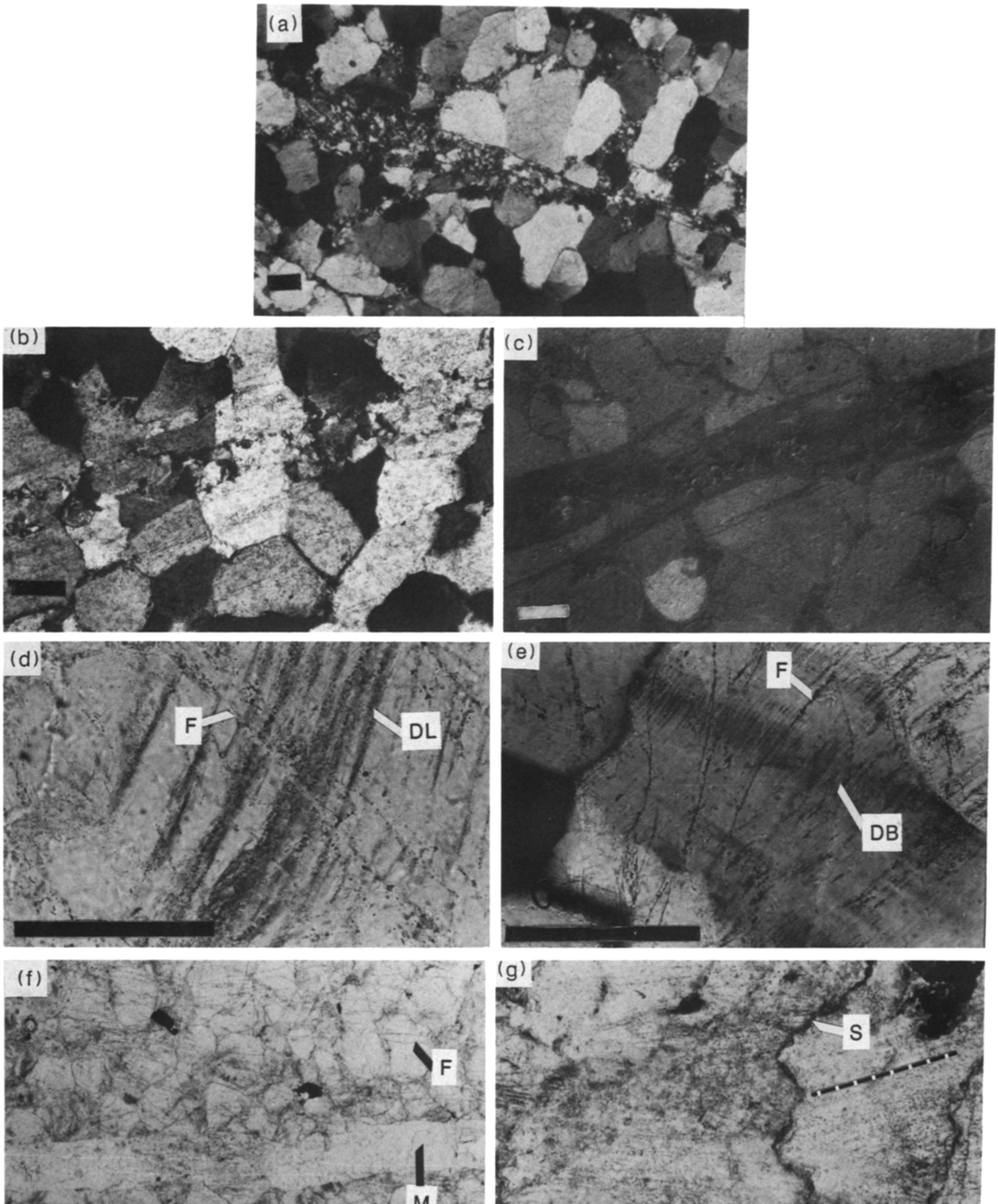

Fig. 3. Microstructures and microstructural relations in the Tuscarora Sandstone. (a) Cataclastic band; (b) mortar texture in linear band with crossed polars; (c) same texture in cathodoluminescence; (d) FIPs (F) cutting deformation lamellae (DL); (e) FIPs (F) passing through deformation band (DB) undeflected; (f) inclusion-free microvein (M) parallel to FIPs (F) in plane light; and (g) stylolite (S) cutting FIPs. Note that the block on the right has been rotated along bounding solution surfaces so that the FIPs (parallel to dashed lines) are discordant to those in the rest of sample. Scale bar in each photomicrograph is 0.1 mm.

Table 1. Relative age relationships between microstructures and association with regional events

Event		Microstructures
Roof Sequence	Duplex	
Compaction	Compaction	Sutured grains, stylolites
Layer-parallel shortening	Layer-parallel shortening	Deformation lamellae and bands, undulatory and patchy extinction
	Ramp formation	FIPs, microveins, cataclastic bands
Folding during emplacement of blind thrusts		Deformation lamellae and bands, FIPs, and microveins
Overturning of NW fold limbs		FIPs, microveins, cataclastic bands, sutured grains, stylolites

northwestern macro-anticlinal fold limbs (4 in Fig. 1b) and in steeply-dipping southeastern fold limbs. Their strike-parallel, bedding-normal geometry indicates that they accommodated dip-parallel extension. These sites also contain the second generation of solution surfaces, which accommodated bedding-normal (subhorizontal) shortening. Locally, this solution outlived fracturing as described above.

The progression of tectonic microstructures present in the Tuscarora is common in a wide variety of structural settings including other thrust belts (Knipe 1989). In the high level sheets of the Moine thrust, dislocation flow was followed by microfracturing then pressure solution (Knipe 1990). Dislocation flow at low temperatures, where climb is difficult, causes work-hardening which can lead to brittle failure (Knipe 1989). Microfracturing and pressure solution can alternate as the strain rate fluctuates, which appears to be the case in the Tuscarora where FIPs and microveins are cut by stylolites and vice versa. As tectonism wanes, pressure solution may record the last increments of deformation (Knipe 1990).

Microstructural abundances

Microstructural abundances showed considerable variation in the samples studied. This variation could be due to deformation being partitioned heterogeneously on a bed or outcrop scale (local effects) or to variations in differential stress magnitude, strain rate, pressure, temperature and deformational history related to different structural locations (regional effects). Because the Tuscarora Sandstone is compositionally uniform and has a simple regional geometry that is generally uncomplicated by mesoscopic folds and faults (Fig. 1b), microscale deformation should be homogeneous at the outcrop scale. This appears to be the case in a detailed study of a single outcrop from the transition zone where the variation in microstructural abundances was found to be much less than that for all samples in this study. Standard deviations for most microstructure abundances are 30–50% of the regional values (J. Bell 1992, personal communication). Therefore, we believe that the variations observed in this study are dominated by regional, not local effects.

Microstructures from dislocation flow are the most common (Fig. 4). However, if undulatory and patchy extinction are excluded because they could be inherited, the most common Alleghanian microstructures in the Tuscarora Sandstone are microfractures, indicating significant brittle behavior in the quartz arenite during deformation. Deformation bands and lamellae from dislocation flow are the second-most common and pressure solution is the least represented mechanism in the microstructural suite. Slightly more than 25% of the grains lack microstructures, indicating some grain-scale heterogeneity in deformation behavior.

The occurrence of certain microstructures was found to be correlated to that of other microstructures (Table 2). Using a t-test on correlations determined by linear regression, significant positive correlations were found between dislocation flow microstructures (undulatory extinction, deformation lamellae and bands) and between brittle microstructures (FIPs, microveins and cataclastic bands). This further strengthens the argument that these microstructures formed *in situ* and are not inherited. Significant correlations were also found between microstructural abundances and certain compositional or textural parameters (Table 2). The strong positive correlation between pressure solution microstructures and the amount of clay matrix is consistent with the well known effect of clay on pressure solution (e.g. Weyl 1959, Rutter 1983). Grain size showed a positive correlation to both patchy extinction and FIPs indicating that larger grains are more likely to have these

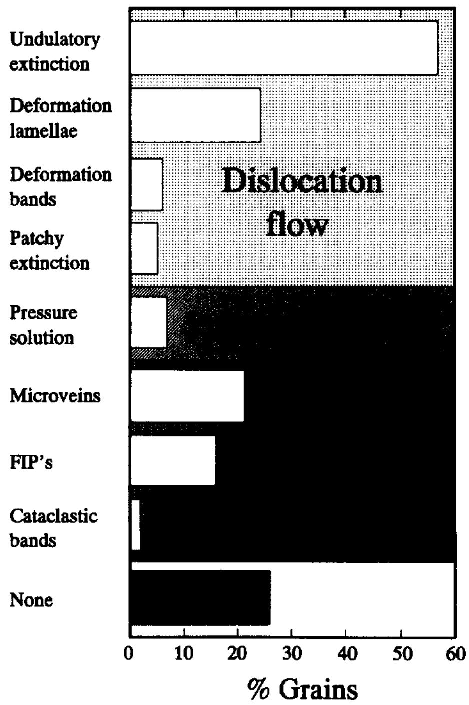

Fig. 4. Histogram showing abundances of microstructures in the Tuscarora Sandstone.

Table 2. Correlation matrix for microstructures, composition and textural parameters. Bold face indicates correlation coefficient is significant at the 95% confidence level

	Undulatory extinction	Deformation lamellae	Deformation band	Patchy extinction	Pressure solution	FIP	Microvein	Cataclastic band	None	% Matrix	Grain size	% Cement
Undulatory extinction	1											
Deformation lamellae	**0.524**	1										
Deformation band	**0.546**	**0.506**	1									
Patchy extinction	−0.113	−0.205	−0.183	1								
Pressure solution	0.197	0.034	−0.050	−0.037	1							
FIP	**0.369**	−0.078	0.210	0.183	−0.115	1						
Microvein	**0.336**	−0.153	0.174	−0.003	−0.119	**0.670**	1					
Cataclastic band	**0.314**	−0.051	−0.026	0.012	−0.042	**0.311**	**0.534**	1				
None	**−0.858**	**−0.574**	**−0.426**	−0.028	−0.253	**−0.550**	**−0.431**	**−0.343**	1			
% Matrix	0.111	−0.034	−0.043	−0.070	**0.869**	−0.150	−0.073	−0.136	−0.252	1		
Grain size	0.180	0.079	0.098	**0.450**	0.084	**0.501**	0.242	0.146	**−0.350**	0.205	1	
% Cement	0.053	−0.044	0.104	0.011	0.117	−0.181	−0.186	−0.246	0.084	0.095	−0.087	1

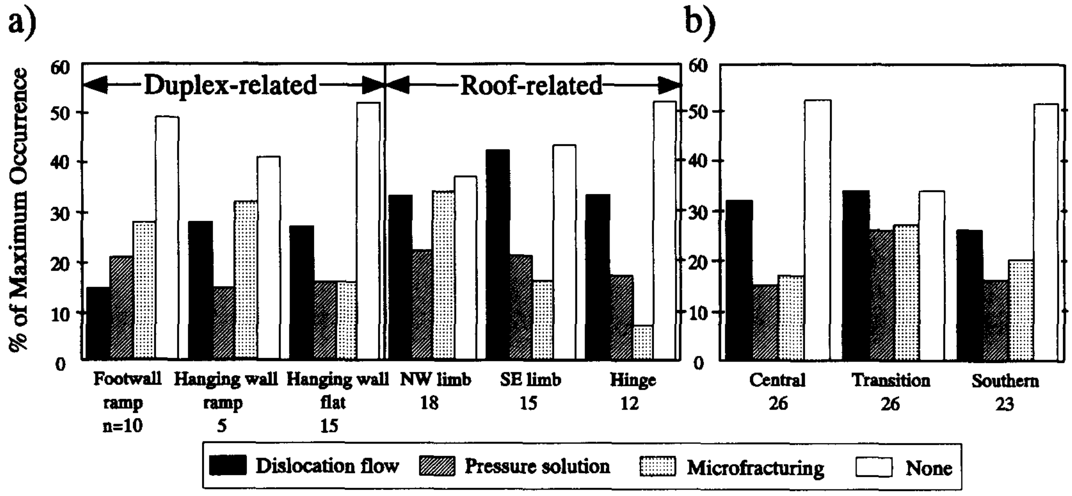

Fig. 5. Deformation mechanism occurrences for samples grouped by: (a) structural location; (b) regional location relative to the central and southern Appalachians.

features. No correlation was found between the amount of cement and any microstructure.

To determine if microstructural development was controlled by structural setting, samples were classified into one of six locations: (1) thrust footwall ramp; (2) thrust hanging-wall ramp; (3) SE-dipping hanging-wall flat; (4) northwestern fold limb; (5) southeastern fold limb; and (6) fold hinge. The first three locations are duplex-related and the last three are roof-related. This classification allows comparisons to be made between thrust system and roof, as well as between the six locations individually.

The variation between locations of the three deformation mechanisms was assessed by grouping microstructures according to their respective deformation mechanism (Fig. 5). Again, undulatory and patchy extinction were not included in dislocation flow due to the uncertainty as to their origin. The occurrence of each mechanism in a given location is expressed as a percentage of the maximum abundance of that mechanism for all locations. This allows comparison of the importance of a mechanism between locations, but not between different mechanisms at a single location. Although the relative occurrence of different mechanisms is an indication of the relative importance of each mechanism at a given location, it should not be used as a quantitative measure of how the strain is partitioned into different mechanisms.

Table 3. Probability of equivalency of deformation mechanisms between groups from one-way ANOVA (Analysis of Variance). Groups are significantly different at the 95% confidence level if $P \leq 0.05$

	Grouped by: Structural position	Roof vs duplex	Regional location
Dislocation flow	0.04	0.007	0.30
Pressure solution	0.96	0.57	0.20
Microfracturing	0.01	0.77	0.28
None	0.32	0.24	0.006

Using one-way ANOVA (Analysis of Variance), the probability of equivalency between groups was calculated for each mechanism (Table 3). The six structural locations were significantly different at the 95% confidence level ($P \leq .05$) with respect to dislocation flow and microfracturing. The groups were somewhat different for the none category and nearly identical for pressure solution. When grouped by roof vs duplex, only dislocation flow differed significantly between groups at the 95% confidence level.

The occurrence of dislocation flow is clearly different in the six structural locations as well as in the roof vs the duplex (Table 3), with roof-related locations having experienced more dislocation flow (Fig. 5a). Because the paleotemperatures discussed earlier do not vary significantly over the region, the increased occurrence of dislocation flow can be attributed to greater differential stresses in the roof during layer-parallel shortening. Competent units in the roof sequence such as the Tuscarora Sandstone are likely to be load-bearing during layer-parallel shortening. Once the unit is segmented, as in the duplex, it would no longer support high loads and hence, dislocation flow would cease to be important. If these microstructures are related to layer-parallel shortening as argued above, then the roof sequence accommodated greater layer-parallel shortening than the blind thrust system as is commonly the case in blind thrust systems (Dunne & Ferrill 1988).

The equivalency of pressure solution between the six structural locations and roof vs duplex shows that the entire region experienced a similar amount of pressure solution (Table 3, Fig. 5a). With the exception of some late pressure solution in steep fold limbs, all pressure solution is compaction-related. Couzens *et al.* (1993) found that finite strains in the same samples used in this study are dominated by compaction and that the most successful strain factorization models were those with a uniform compaction of 30–35% volume loss across the area.

The difference in microfracturing is significant between the six locations, but not between the roof vs the duplex (Table 3). Microfracturing is less common in hanging-wall flats, southeastern fold limbs, and fold hinges and about twice as common on average in the steeply-dipping beds adjacent to footwall and hanging wall ramps, and in northwestern fold limbs, where it accommodated dip-parallel extension.

Samples were also classified by regional location in the central, southern, or transition zone of the Appalachians (Fig. 5b). One-way ANOVA results show that the three locations differ significantly at the 95% confidence level with respect only to the none category of mechanisms (Table 3). From this, it can be said that samples from the transition zone have the smallest occurrence of grains with no microstructures (i.e. they are the most deformed). Although not significant at the 95% confidence level (Table 3), it also appears that the central Appalachians have more dislocation flow and less pressure solution and microfracturing than the southern Appalachians (Fig. 5b). If the deformational history proposed in Table 1 is correct, the overlap of central and southern Appalachian deformations would result in two phases of brittle deformation in the transition zone. This could explain the increased diversity of microfractures in the transition zone as illustrated by the southeastern limb of the Rich Patch anticline (RPA, Fig. 1a). Samples from this fold limb (C3 and D6a, Fig. 6) contain a microfracture population that is more diverse in style and orientation than those from similar structural positions in either the central (A8, Fig. 6) or southern (H5, Fig. 6) Appalachians. The additional microfractures may result from a second brittle deformation, where central Appalachian deformation developed in quartz arenites that were strain-hardened by the older southern Appalachian deformation. Further evaluation of the overlap of deformation awaits an analysis of microstructure orientations in the three regions.

CONCLUSIONS

(1) The quartz arenite of the Tuscarora Sandstone developed the same sequence of deformation mechanisms for similar pressure–temperature conditions in both the blind thrust system and roof sequence: pressure solution during sedimentary compaction; dislocation flow during layer-parallel shortening; and localized microfracturing with limited solution near major thrust ramps and in steeply-dipping fold limbs.

(2) The greater abundance of dislocation flow microstructures in the roof, and their correlation to layer-parallel shortening, indicates that the Tuscarora Sandstone underwent greater layer-parallel shortening in the roof than in the duplex. Therefore, the roof absorbed some of the macroscale shortening from the emplacement of the underlying blind thrust system by microscale shortening.

(3) The greatest regional accumulation of microstruc-

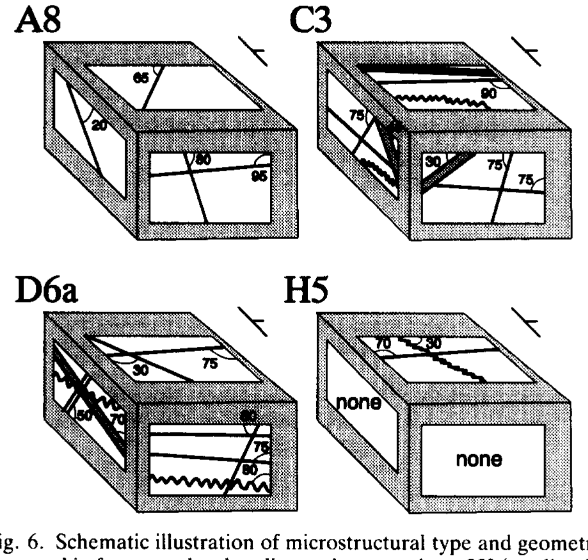

Fig. 6. Schematic illustration of microstructural type and geometries observed in four samples that dip southeast at about 23° (small strike/dip symbols show geometry). A8 is in the roof sequence of the central Appalachians; C3 and D6a are from the transition zone; and H5 is from a duplex horse in the southern Appalachians. Each block represents a sample and three white rectangles represent mutually-perpendicular thin sections. Solid lines—FIPs; closely spaced, parallel solid lines—abundant FIPs; shaded bands—cataclastic bands; wavy lines—solution surfaces. Features do not connect between some faces in a given block because some microstructures were not extensive enough to transect more than one thin section.

tures in the roof sequence occurred at the transition zone between the southern and central Appalachian foreland, which is consistent with older southern Appalachian deformation being overprinted by younger central Appalachian deformation. The overprint was manifested in some structural locations by greater diversity and abundance of microfractures, possibly indicating the quartz arenite was strain-hardened by the first deformation.

Acknowledgements—This work was funded by NSF grant EAR-8915949 to Dunne and Onasch. Brent Couzens and Randy Glass assisted in the field work and sample preparation. The generosity of Art Schultz and Jerry Bartholomew, who shared data from maps in-press, is greatly appreciated. The manuscript benefited from thorough reviews by Richard Groshong, Jr and an anonymous reviewer.

REFERENCES

Amato, R. V. 1974. Geology of the Salem Quadrangle, Virginia. *Virginia Div. Miner. Resourc. Rep. Invest.* **37**.

Aydin, A. & Johnson, A. M. 1978. Developments of faults as zones of deformation bands and as slip surfaces in sandstone. *Pure & Appl. Geophys.* **116**, 932–942.

Bartholomew, M. J. 1981. Geology of the Roanoke and Stewartsville Quadrangles, Virginia. *Virginia Div. Miner. Resourc. Publ.* **34**.

Bartholomew, M. J. 1987. Structural evolution of the Pulaski thrust system, southwestern Virginia. *Bull. geol. Soc. Am.* **99**, 491–510.

Bartholomew, M. J. & Lowry, W. D. 1979. Geology of the Blacksburg Quadrangle, Virginia. *Virginia Div. Miner. Resourc.* Publ. **14**.

Bartholomew, M. J. & Schultz, A. P. *et al.* In press. *Geologic Map of Radford 1:100,000 sheet.* United States Geologic Survey, Reston, VA.

Bick, K. F. 1960. Geology of the Lexington Quadrangle, Virginia. *Virginia Div. Miner. Resourc. Rep. Invest.* **1**.

Bick, K. F. 1962. Geology of the Williamsville Quadrangle, Virginia. *Virginia Div. Miner. Resourc. Rep. Invest.* **2**.

Blenkinsop, T. G. & Rutter, E. H. 1986. Cataclastic deformation of quartzites in the Moine thrust system. *J. Struct. Geol.* **8**, 664–681.

Boyer, S. E. & Elliott, D. 1982. Thrust systems. *Bull. Am. Ass. Petrol. Geol.* **66**, 1196–1230.

Butts, C. 1940. Geology of the Appalachian Valley in Virginia. *Virginia Div. Miner. Resourc. Bull.* **52**.

Calver, J. L. 1960. Geology and mineral resources of Rockingham County. *Virginia Div. Miner. Resourc. Bull.* **76**.

Colton, G. W. 1970. The Appalachian basin—Its depositional sequences and their geologic relationships. In: *Studies of Appalachian Geology: Central and Southern* (edited by Fisher, G. W., Pettijohn, F. J., Read, J. C., Jr & Weaver, K. N.). Wiley- Interscience, New York, 5–47.

Cooper, B. N. 1944. Geology and mineral resources of the Burkes Garden Quadrangle, Virginia. *Virginia Div. Miner. Resourc. Bull.* **60**.

Couzens, B. A., Dunne, W. M., Onasch, C. M. & Glass, R. 1993. Strain variations and three-dimensional strain factorization at the transition from the southern to central Appalachians. *J. Struct. Geol.* **15**, 451–464.

Dean, S. L., Kulander, B. R. & Skinner, J. M. 1988. Structural chronology of the Alleghanian orogeny in southeastern West Virginia. *Bull Geol. Soc. Am.* **100**, 299–310.

Diecchio, R. J. 1985. Post-Martinsburg Ordovician stratigraphy of Virginia and West Virginia. *Virginia Div. Miner. Resourc. Publ.* **57**.

Dunne, W. M. & Ferrill, D. A. 1988. Blind thrust systems. *Geology* **16**, 33–36.

Elliott, D. 1976. The energy balance and deformation mechanisms of thrust sheets. *Phil. Trans. R. Soc. Lond.* **A283**, 289–312.

Epstein, A. G., Epstein, J. B. & Harris, L. D. 1977. Conodont color alteration—an index to organic metamorphism. *Prof. Pap. U.S. geol. Surv.* **995**.

Evans, M. A. & Dunne, W. M. 1991. Strain factorization and partitioning in a foreland thrust sheet. *J. Struct. Geol.* **13**, 13–25.

Fairbairn, H. W. 1941. Deformation lamellae in quartz from the Ajibik Formation, Michigan. *Bull. geol. Soc. Am.* **52**, 1265–1278.

Ferrill, D. A. & Dunne, W. M. 1989. Cover deformation above a blind duplex: an example from West Virginia, U.S.A. *J. Struct. Geol.* **11**, 421–431.

Geiser, P. A. 1988a. Mechanisms of thrust propagation: some examples and implications for the analysis of overthrust terranes. *J. Struct. Geol.* **10**, 829–845.

Geiser, P. A. 1988b. The role of kinematics in the construction and analysis of geological cross sections in deformed terranes. In: *Geometries and Mechanisms of Thrusting, With Special Reference to the Appalachians* (edited by Mitra, G. & Wojtal, S.). *Spec. Pap. geol. Soc. Am.* **222**, 47–75.

Geiser, P. A. & Engelder, T. 1983. The distribution of layer-parallel shortening fabrics in the Appalachian foreland of New York and Pennsylvania; evidence for two, non-coaxial phases of Alleghanian orogeny. In: *Contributions to the Tectonics and Geophysics of Mountain Chains* (edited by Hatcher, R. D., Williams, H. & Zeitz, I.). *Mem. geol. Soc. Am.* **158**, 161–175.

Gray, M. B. & Mitra, G. 1991. Spatial and temporal aspects of progressive deformation in a blind fold and thrust belt: Pennsylvania anthracite region, USA. *Mitt. Geol. Inst. ETH Zurich, N.F.* **239b**, 24–25.

Groshong, R. H. Jr. 1988. Low-temperature deformation mechanisms and their interpretations. *Bull. geol. Soc. Am.* **100**, 1329–1360.

Harris, A. G. 1970. Conodont color alteration, an organo-mineral metamorphic index, and its application to Appalachian Basin geology. In: *Aspects of Diagenesis* (edited by Scholle, P. A. & Schluger, P. R.). *Spec. Publ. Soc. econ. Petrol. Miner.* **26**, 3–16.

Hirth, G. & Tullis, J. 1992. Dislocation creep regimes in quartz aggregates. *J. Struct. Geol.* **14**, 145–159.

Houseknecht, D. W. 1988. Intergranular pressure solution in four quartzose sandstones. *J. Sedim. Petrol.* **58**, 228–246.

Jamison, W. R. & Stearns, D. W. 1982. Tectonic deformation of Wingate Sandstone, Colorado National Monument. *Bull. Am Ass. Petrol. Geol.* **66**, 2584–2608.

Knipe, R. J. 1989. Deformation mechanisms—recognition from natural tectonites. *J. Struct. Geol.* **1**, 127–146.

Knipe, R. J. 1990. Microstructural analysis and tectonic evolution in thrust systems: examples from the Assynt region of the Moine thrust zone, NW Scotland. In: *Deformation Processes in Minerals, Ceramics, and Rocks* (edited by Barber, D. J. & Meredith, P. G.). *Spec. Publ. Miner. Soc.* **1**.

Koch, G. S., Jr & Link, R. F. 1970. *Statistical Analysis of Geological Data, Volume* 1. John Wiley & Sons, New York.

Kozak, S. J. 1965. Geology of Millboro Quadrangle, Virginia. *Virginia Div. Miner. Resourc. Rep. Invest.* **8**.

Kozak, S. J. 1970. Geology of the Elliott Knob, Deerfield, Craigsville, and Augusta Springs Quadrangles, Virginia. *Virginia Div. Miner. Resourc. Rep. Invest.* **21**.

Kreisa, R. D. & Springer, D. A. 1987. Lithostratigraphy and biostratigraphy of the Martinsburg Formation in southwestern Virginia, with descriptive sections. In: *Contributions to Virginia Geology—V. Virginia Div. Miner. Resourc. Publ.* **74**, 33–54.

Kulander, B. R. & Dean, S. L. 1986. Structure and tectonics of the central and southern Appalachian Valley and Ridge and Plateau provinces, West Virginia and Virginia. *Bull. Am. Ass. Petrol. Geol.* **70**, 1674–1684.

Kulander, B. R. & Dean, S. L. 1988. The North Mountain–Pulaski fault system and related thrust sheet structure. In *Geometries and Mechanisms of Thrusting, with Special Reference to the Appalachians* (edited by Mitra, G. & Wojtal, S.). *Spec. Pap. geol. Soc. Am.* **222**, 107–117.

Lewis, S. E. & Hower, J. C. 1990. Implications of thermal events on thrust emplacement sequence in the Appalachian fold and thrust belt: some new vitrinite reflectance data. *J. Geol.* **98**, 927–942.

Lloyd, G. E. & Knipe, R. J. 1992. Deformation mechanism accommodating faulting of quartzite under upper crustal conditions. *J. Struct. Geol.* **14**, 127–143.

Marshak, S. & Engelder, T. 1985. Development of cleavage in limestones of a fold–thrust belt in eastern New York. *J. Struct. Geol.* **7**, 345–359.

McGuire, O. S. 1970. Geology of the Eagle Rock, Strom, Oriskany, and Salisbury Quadrangles, Virginia. *Virginia Div. Miner. Resourc. Rep. Invest.* **24**.

McGuire, O. S. 1976. Geology of the Daleville Quadrangle, Virginia. *Virginia Div. Miner. Resourc. Rep. Invest.* **42**.

Meyer, T. J. & Dunne, W. M. 1990. Multi-stage deformation of cover limestones above a blind thrust system: An example from the central Appalachians. *J. Geol.* **98**, 108–117.

Mitra, S. 1987. Regional variations in deformation mechanisms and structural styles in the central Appalachian orogenic belt. *Bull. geol. Soc. Am.* **98**, 569–590.

Narahara, D. K. and Wiltschko, D. 1986. Deformation in the hinge region of a chevron fold, Valley and Ridge Province, central Pennsylvania. *J. Struct. Geol.* **8**, 157–168.
Nicolas, A. & Poirier, J. P. 1976. *Crystalline Plasticity and Solid State Flow in Metamorphic Rocks*. New York, John Wiley & Sons.
Onasch, C. M. 1984. Petrofabric test of viscous folding theory. *Tectonophysics* **106**, 141–153.
Onasch, C. M. 1990. Microfractures and their role in deformation of a quartz arenite from the central Appalachian foreland. *J. Struct. Geol.* **12**, 883–894.
Onasch, C. M. & Canich, M. 1976. Dynamic analysis of the Laurel Creek Reservoir area. In: *Second Int. Conf. on New Basement Tectonics: Field Guide to Lineaments and Fractures in Central Pennsylvania* (edited by Gold, D. & Parizek, R.), 29–35.
Perry, W. J., Jr. 1968. Dynamic analysis of quartz from a major asymmetric fold in West Virginia. *Geol. Soc. Am. Abs. w. Prog.*, 233–234.
Perry, W. J., Jr. 1978. Sequential deformation in the central Appalachians. *Am. J. Sci.* **278**, 518–542.
Rader, E. K. 1967. Geology of the Staunton, Churchville, Greenville, and Stuarts Draft Quadrangles, Virginia. *Virginia Div. Miner. Resourc. Rep. Invest.* **12**.
Rader, E. K. 1969. Geology of the Stokesville and Parnassus Quadrangles, Virginia. *Virginia Div. Miner. Resourc. Rep. Invest.* **19**.
Reger, D. B. 1931. Randolph County. *West Virginia Geol. & Econ. Surv.*
Reger, D. B. & Price, P. 1926. Mercer, Monroe, and Summers Counties. *West Virginia Geol. & Econ. Surv.*
Rodgers, J. 1970. *The Tectonics of the Appalachians*. Wiley-Interscience, New York.
Rutter, E. H. 1983. Pressure solution in nature, theory and experiment. *J. geol. Soc. Lond.* **140**, 725–740.
Sanderson, D. J. 1982. Models of strain variation in nappes and thrust sheets: A review. *Tectonophysics* **88**, 201–233.
Schultz, A. P., Stanley, C. B., Gathright, T. M., II, Rader, E. K., Bartholomew, M. J., Lewis, S. E. & Evans, N. H. 1986. Geologic map of Giles County, Virginia. *Virginia Div. Miner. Resourc. Publ.* **69**.
Sibley, D. F. & Blatt, H. 1976. Intragranular pressure solution and cementation of the Tuscarora orthoquartzite. *J. sedim. Petrol.* **46**, 881–896.
Spencer, E. W. 1964. Geology of the Natural Bridge, Sugarloaf Mountain, Buchanan, and Arnold Valley Quadrangles, Virginia. *Virginia Div. Miner. Resourc. Rep. Invest.* **13**.
Sprunt, E. S. & Nur, A. 1979. Microcracking and healing in granites: New evidence from cathodoluminescence. *Science* **205**, 495–497.
Stamatakos, J. & Kodama, K. P. 1991. Grain-scale strains and remanence rotation in redbeds. *Mitt. Geol. Inst. ETH Zurich, N. F.* **239b**, 70–71.
Thompson, R. I. 1979. A structural interpretation across part of the northern Rocky Mountains, British Columbia, Canada. *Can. J. Earth Sci.* **16**, 1228–1241.
Tilton, J. L., Prouty, W. F. & Price, P. H. 1927. Pendleton County. *West Virginia Geol. & Econ. Surv.*
Tullis, J. & Yund, R. A. 1985. Dynamic recrystallization of feldspar: A mechanism for ductile shear zone formation. *Geology*, **13**, 238–241.
Tullis, J. A. & Yund, R. A. 1987. Transition from cataclastic flow to dislocation creep of feldspar: Mechanisms and microstructures. *Geology* **15**, 606–609.
Van Der Plas, L. & Tobi, A. C. 1965. A chart for judging the reliability of point counting results. *Am. J. Sci.* **263**, 87–90.
Woodward, N. B. 1985. Valley and Ridge thrust belt; balanced structural sections, Pennsylvania to Alabama. *Univ. Tennessee, Stud. Geol.* **12**.
Woodward, N. B., Gray, D. R. & Spears, D. B. 1986. Including strain in balanced cross-sections. *J. Struct. Geol.* **8**, 313–324.
Wu, S. & Groshong, R. H. Jr. 1991. Low-temperature deformation of sandstone, southern Appalachian fold-thrust belt. *Bull. geol. Soc. Am.* **103**, 861–875.
Weyl, P. K. 1959. Pressure solution and the force of crystallization—a phenomenological theory. *J. geophys. Res.* **64**, 2001–2025.